Concentration, size, mean lifetime, and noise effects on image quality in luminescence optical tomography

J. Chang[1], H. L. Graber[2], R. L. Barbour[1,2]

Department of Pathology[1], and Program in Physiology and Biophysics[2]
SUNY Health Science Center at Brooklyn, Brooklyn

Abstract

The impact of background lumiphore in luminescence optical tomography is examined. To demonstrate its effects, numerical simulations were performed to calculate the diffusion–regime limiting form of forward–problem solutions for a specific test medium. Image reconstructions were performed using a CGD algorithm with a rescaling technique and positivity constraints. In addition, we develop a modification to the basic algorithm that makes use of the maximum possible concentration in order to estimate the background concentration, and show that it improves image quality when background lumiphore is present. We conclude that the usual measure of background lumiphore's effect, which is the target-to-background lumiphore concentration ratio, is not adequate to define the contribution from the background lumiphore. The reason for this is that image quality is also a function of target size and location. An alternative measure that we find superior is described. The results indicate that the improved algorithm yields better image quality for low target–to–background ratios.

1. Introduction

The use of lumiphore in optical diffusion tomography to enhance the image quality has drawn great interest recently [1,2]. Luminescent compounds play a similar role in optical tomography to that of radiopharmaceutical agents in nuclear medicine, in that both types of molecules actively emit photons from which projection or tomographic images are reconstructed. In an earlier paper [3] we described algorithms we have developed for reconstruction of two useful quantities in luminescence optical tomography. The first of these is $\gamma\sigma_{T,1\to 2}N_0$, that is, the product of the lumiphore's quantum yield, microscopic cross section, and concentration. The second is the mean lifetime τ. We showed in the earlier study that $\gamma\sigma_{T,1\to 2}N_0$ can be reconstructed from DC (*i.e.*, steady–state, $\omega = 0$) detector readings. If detector readings for at least one $\omega \neq 0$ also are available, then they can in principle be used to reconstruct τ directly, without knowledge of $\gamma\sigma_{T,1\to 2}N_0$. However, for a numerical reason we adopted a "concentration correction" that makes use of the $\gamma\sigma_{T,1\to 2}N_0$ information while reconstructing τ. To implement this correction, the maximum value of each $\gamma\sigma_{T,1\to 2}N_0$ map is first obtained, and any value smaller than a threshold proportional to the maximum is set to zero. This modified $\gamma\sigma_{T,1\to 2}N_0$ map is then used in the calculation of the weight matrix (imaging operator) for the corresponding mean lifetime reconstruction. The examples we presented [3] showed that this concentration correction procedure works well in the absence of background lumiphore. Subsequently, however, we have seen that when background lumiphore is present, the reconstruction results are not satisfactory (see below).

One idea we have pursued in our efforts to deal with the problem just described is to make better use of *a priori* information in our image–reconstruction algorithms. It is well known that the use of *a priori* information is a powerful tool, especially for ill–conditioned problems [4]. Previous studies [5] have demonstrated that positivity constraints and range constraints can effectively improve image quality. However, great care must be taken to use range constraints properly, or they may not provide satisfactory results when background lumiphore is present. Background lumiphore not only significantly increases the detected signal, but also makes it difficult to assign a lower limit to the range constraint. An arbitrary choice of a lower bound (typically zero) is not satisfactory, as shown below in the results section. Thus, a requirement for successful reconstruction is a reasonable estimate of the background lumiphore concentration.

Here we present a new procedure we have developed to improve the reconstruction of concentration and mean lifetime for the case of background lumiphore uniformly distributed in space with a single constant mean lifetime. A

SPIE Vol. 2979 • 0277-786X/97/$10.00

technique is proposed to estimate the background lumiphore concentration (under this assumption of uniform concentration and τ), which is then used to improve the accuracy of the reconstruction.

2. Theory

Detector Readings

The luminescent light detector readings, for a time–harmonic excitation source are related to the properties of the medium and lumiphore by [3,6]

$$\tilde{R} = \int_V \frac{\tilde{\tilde{\phi}}_1 \tilde{\tilde{\phi}}_2^+}{4\pi} \frac{\gamma \sigma_{T,1\to 2} N_0 e^{-j\tan^{-1}\omega\tau}}{\sqrt{1+\omega^2\tau^2}} d^3r \tag{1}$$

where ω is the modulation frequency, τ is the mean lifetime of the lumiphore's excited state, γ is its quantum yield, $\sigma_{T,1\to 2}$ is the microscopic total cross section [cm^2] of the lumiphore, N_0 is the lumiphore concentration, $\tilde{\tilde{\phi}}_1 = \tilde{\tilde{\phi}}(\mathrm{r},\omega)$ is the intensity (fluence rate) [cm^{-2} Hz^{-1}] of the excitation light, and $\tilde{\tilde{\phi}}_2^+ = \tilde{\tilde{\phi}}_2(\mathrm{r},\omega) = \int_{4\pi}\left[\int_V \int_{4\pi} \tilde{\delta}_2' \tilde{G}_2(\mathrm{r},-\Omega;\mathrm{r}',-\Omega';\omega) d\Omega' d^3r'\right] d\Omega$ is the adjoint intensity for the emission light, where $\tilde{\delta}_2' = \tilde{\delta}_2'(\mathrm{r}',\Omega')$ is the detector sensitivity function.

For a point source and point detector, $\tilde{\tilde{\phi}}_1$ and $\tilde{\tilde{\phi}}_2^+$ are the Green's function for light propagating from the source and detector, respectively, to each voxel. That is

$$\tilde{R} = \int_V \frac{1}{4\pi} \frac{e^{-j|\mathrm{r}-\mathrm{r}_s|}}{4\pi|\mathrm{r}-\mathrm{r}_s|^2} \frac{e^{-j|\mathrm{r}-\mathrm{r}_d|}}{4\pi|\mathrm{r}-\mathrm{r}_d|^2} \frac{\gamma \sigma_{T,1\to 2} N_0 e^{-j\tan^{-1}\omega\tau}}{\sqrt{1+\omega^2\tau^2}} d^3r \tag{2}$$

where r_s and r_s are the source and detector locations, and k^x and k^e are the complex wave numbers for the excitation and emission photon density wave.

The Contributions from the Target and Background Lumiphore

When the source and detector are located far from the integration volume of Eq. (2), we can approximate $|\mathrm{r}-\mathrm{r}_s|$ and $|\mathrm{r}-\mathrm{r}_s|$ by, respectively, $|\mathrm{r}_0-\mathrm{r}_s|$ and $|\mathrm{r}_0-\mathrm{r}_s|$ where r_0 is the center of the integration volume (*i.e.*, the far–field approximation). Then the amplitude of the detected signal can be approximated by

$$\tilde{R} \approx \frac{\gamma \sigma_{T,1\to 2} N_0 e^{-j\left(k^x|\mathrm{r}_0-\mathrm{r}_s|+k^e|\mathrm{r}_0-\mathrm{r}_d|\right)} e^{-j\tan^{-1}\omega\tau} V_T}{(4\pi)^3 |\mathrm{r}_0-\mathrm{r}_s|^2 |\mathrm{r}_0-\mathrm{r}_d|^2 \sqrt{1+\omega^2\tau^2}} \tag{3}$$

In general, the detected signal is the sum of the signals from target and from the background lumiphore, that is, $\tilde{R} = \tilde{R}_{Tr} + \tilde{R}_B$, where *Tr* and *B* denote the "target" and "background," respectively. The ratio of contributions from the background and target, $\tilde{R}_B/\tilde{R}_{Tr}$, is a function of the concentration background–to–target ratio, the location of the target, and the size of the target.

3. Reconstruction Algorithm

An new procedure was developed to improve the reconstruction when background lumiphore is present. Here we assume that the background lumiphore is uniformly distributed with a constant concentration and mean lifetime, and the target is an isolated object. Under these assumptions, this algorithm works as follows:

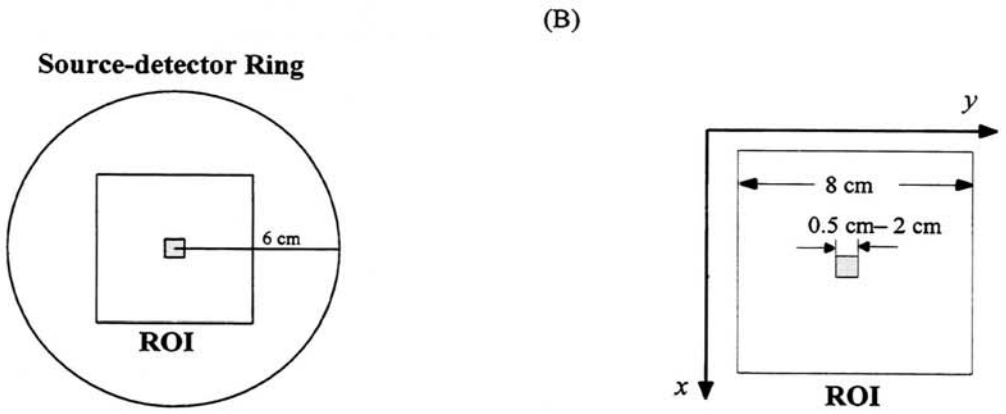

Figure 1. Sketches of phantom structure and source–detector ring used for diffusion computation.

1. Estimate the background lumiphore concentration using the *maximum possible concentration principle* (MPCP).
2. Reconstruct the concentration using an iterative algorithm (*e.g.*, CGD, POCS, SART) with a range constraint where the upper and lower bounds are the maximum possible target concentration and the estimated background lumiphore concentration.
3. Restrict the target volume by setting to zero all voxels where the reconstructed concentration is less than a preselected fraction of the maximum reconstructed concentration.
4. Reconstruct the mean lifetime of the target and background. Here, we sum the weight function over all the background voxels so that the unknowns in this reconstruction are the voxels in the target and in one "lump" background voxel, thereby greatly reducing the dimension of the vector of unknowns.

The *maximum possible concentration principle* is a technique to reasonably estimate the background concentration from the DC detector readings. We assume that the detected signal comes entirely from the background lumiphore. Since the background lumiphore concentration is constant, it is equal to the ratio of a detector reading and the sum of the corresponding weight function over all voxels. An estimate of $\gamma\sigma_{T,1\to 2}N_0$ is obtained for each detector reading, and the lowest of these estimates is used as the lower bound for range constraint. This minimum is the greatest possible background concentration, since any larger value would imply a negative contribution from the target.

4. Methods

Numerical simulations were performed to calculate solutions to the diffusion equations describing the excitation and emission fields. The phantom was an infinite medium with background lumiphore uniformly distributed in an 8.0 × 8.0 cm² square region of interest (ROI) (Figure 1A). This area is discretized into 0.25×0.25 cm² square voxels. The target was a smaller square located at the center of the ROI (Figure 1B). In the four test cases studied, the target size was: (A) 0.5 cm×0.5 cm, (B) 1.0 cm×1.0 cm, (C) 1.5 cm×1.5 cm, and (D) 2.0 cm×2.0 cm. The macroscopic cross sections for both excitation and emission lights were $\mu_s = 1{,}000\ \mathrm{m}^{-1}$ and $\mu_a = 3\ \mathrm{m}^{-1}$. The absorption cross section introduced by the lumiphore was $\mu_T = 0.01\ \mathrm{m}^{-1}$. The mean lifetimes of the background and target lumiphore were 10^{-9} s and 5×10^{-9} s, respectively. Diffusion equation solutions were computed for DC illumination and for time–harmonic illumination at a modulation frequency of 100 MHz. These computations supplied the required information for reconstruction of the product of concentration, microscopic cross section and quantum yield, and of mean lifetime. Different levels of Gaussian noise (defined as the ratio of the signal mean to the noise standard deviation) were also added to the detector readings. Image reconstructions were performed using the original and improved algorithms, and were terminated after 10,000 iterations.

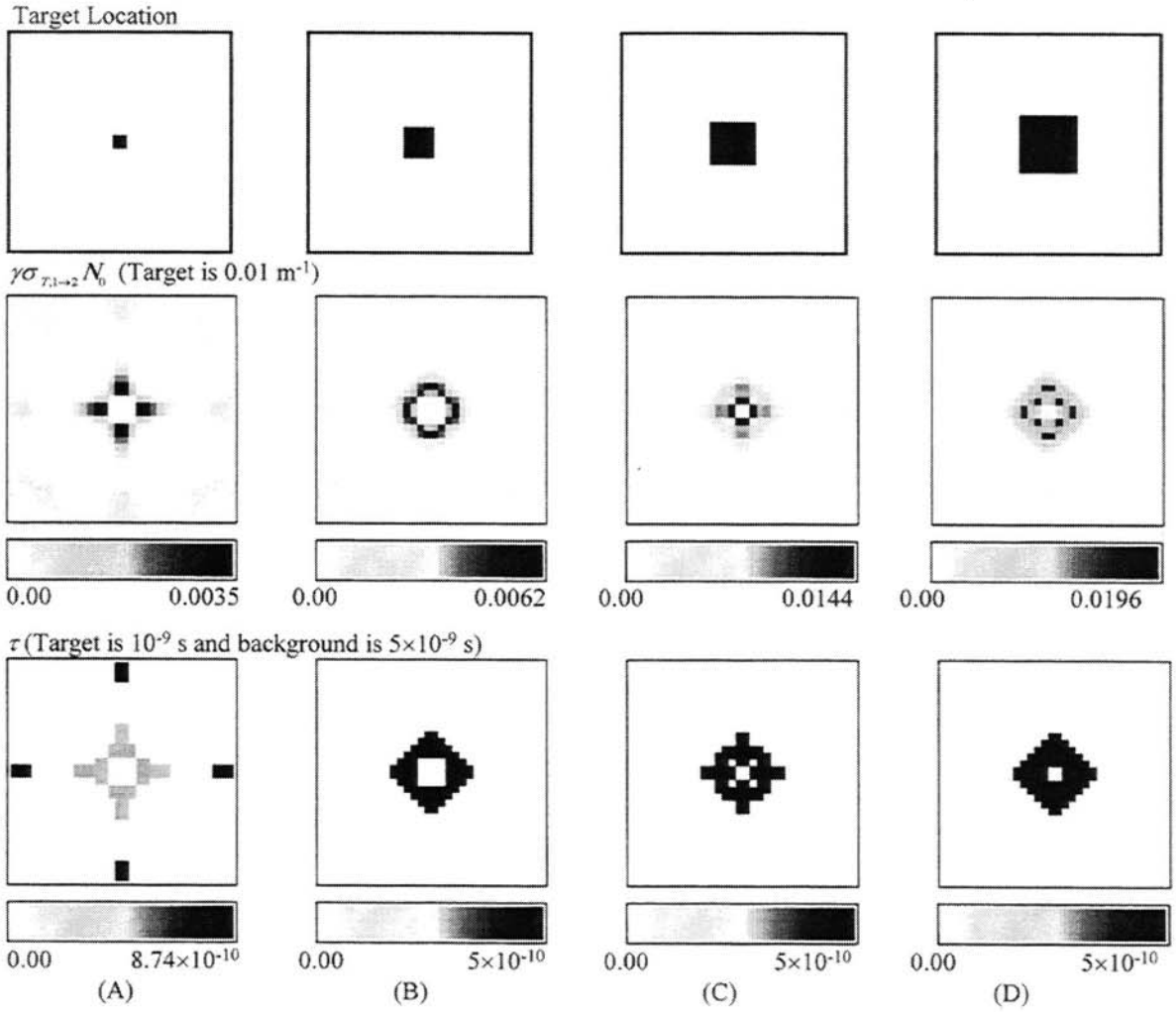

Figure 2. Reconstruction results with background–to–target ratio of 0.01 and different target sizes, using the previously described algorithm [3] with constraints.

5. Results

Figure 2 shows the reconstructed concentration and mean lifetime when the background–to–target lumiphore concentration ratio was 0.01, for different target sizes: (A) 0.5 cm×0.5 cm, (B) 1.0 cm×1.0 cm, (C) 1.5 cm×1.5 cm, and (D) 2.0 cm×2.0 cm, using the previously described algorithm [3] with a positivity constraint on the concentration and a 5×10^{-10} s to 5×10^{-9} s range constraint on the mean lifetime. Figure 3 demonstrates the reconstruction results from the same sets of data as used for Figure 2, using the improved algorithm. The concentration was constrained to lie between the maximum target concentration (0.05 m^{-1}) and estimated background concentration (selected by the algorithm.) (A) 0.5 cm×0.5 cm, (B) 1.0 cm×1.0 cm, (C) 1.5 cm×1.5 cm, and (D) 2.0 cm×2.0 cm. Figure 4 illustrates the reconstruction results when the background–to–target lumiphore concentration ratio was 0.2 for targets of different sizes, using the improved algorithm with the same constraints as in the preceding case. (A) 0.5 cm×0.5 cm, (B) 1.0 cm×1.0 cm, (C) 1.5 cm×1.5 cm, and (D) 2.0 cm×2.0 cm. A comparison of reconstructed $\gamma\sigma_{T,1\to2}N_0$ using the previous and improved algorithms with background–to–target concentration ratio of 0.01 is shown in Figure 5. The target size is 1.0 cm×1.0 cm. Figure 6. demonstrates the reconstruction results with a fixed background–to–target

ratio of 0.01 and fixed target size of 2.0 cm×2.0 cm, with different levels of added noise (1.0%, 3.0%, 5.0%, and 10.0%) and using the improved algorithm with constraints.

6. Discussions and Conclusion

In an earlier report [3] we described an algorithm that sequentially computes $\gamma\sigma_{T,1\to2}N_0$ and τ using DC and AC data. These conditions were selected based on the expected source–frequency–dependence of detector sensitivity to changes in these quantities. In the presence of background lumiphore, however, the original algorithm failed to provide accurate quantitative results for either concentration or mean lifetime (Figure 2), even when a positivity constraint was used. The algorithm set many voxels to zero while reconstructing $\gamma\sigma_{T,1\to2}N_0$, instead of generating the uniform background we expected. This is due to the underdeterminedness of the weight matrix, which has infinitely many left–inverses, and that a uniform distribution does not lie on the fastest–converging path chosen by the algorithm. For a fixed target–to–background lumiphore concentration ratio, more accurate reconstructions were obtained for larger targets. This is consistent with our theoretical finding in Section 2 that the background–to–target ratio itself is not enough to evaluate the difficulty of an image reconstruction, and the target size should be considered as well. In addition, the far–field approximation made in deriving Eq. (3) is valid only for sources and detectors located far from the ROI. The results in Fig. 2 demonstrate that the same relation also holds qualitatively for near–field sources and detectors.

The reconstructions shown in Figure 3, obtained from the new algorithm, show significant improvement over those obtained from the previous algorithm. Good results were seen even for a background–to–target ratio of 0.2, as shown in Figure 4. The correlation of image quality with target size is not significant, or even becomes negative,

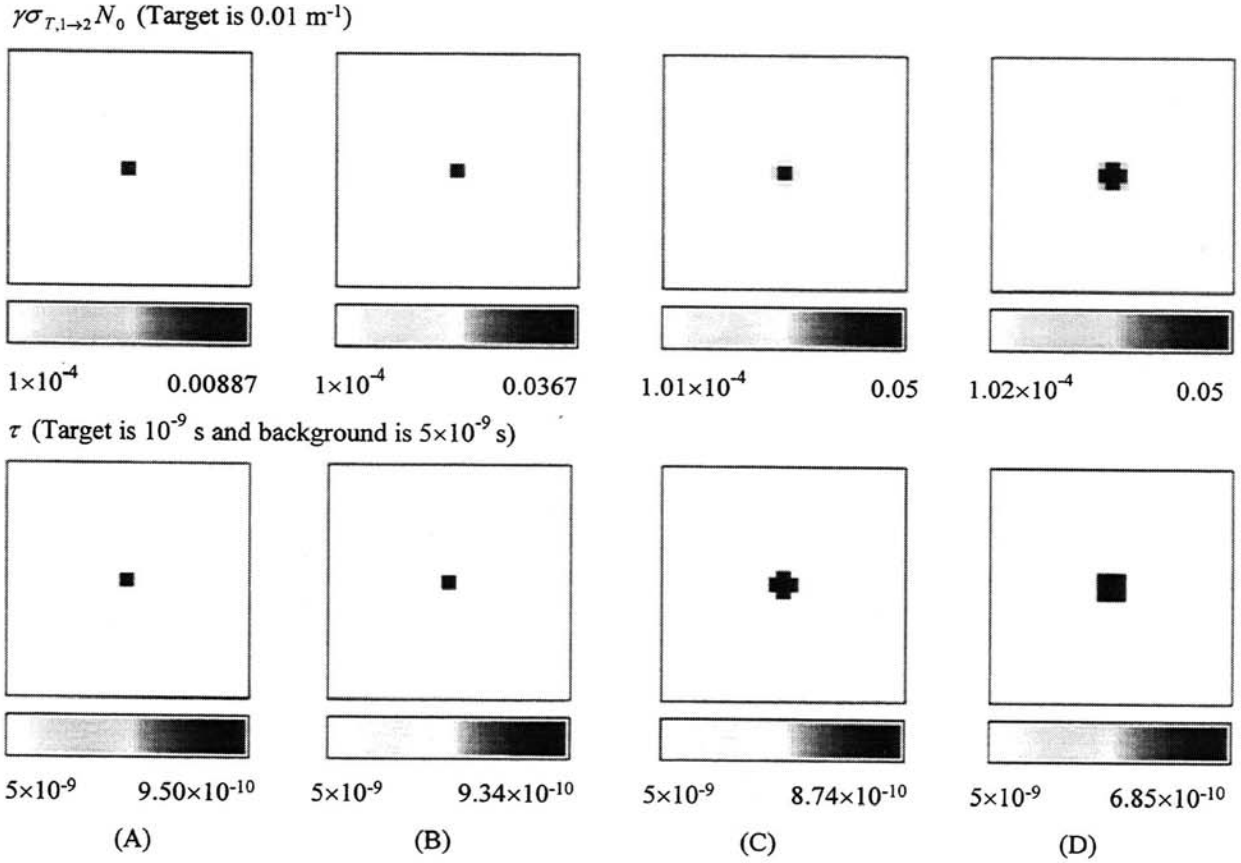

Figure 3. Reconstruction results with background–to–target ratio of 0.01 and different target sizes, using the improved algorithm with constraints.

because the background concentration is accurately estimated using the maximum possible concentration principle. The size of the target, however, is underestimated for larger targets (Figure 3B, 3C, 3D), while the quantitative values are overestimated. This likely is a consequence of the underdeterminedness of the weight matrix and can be remedied by using a technique such as Tikhonov regularization [7]. In addition, the reconstructed mean lifetime is less accurate for larger objects because of the underestimated target size. The reversed correlation between the image quality and target size can be explained as follows. The presence of the target increases the detector reading appreciably above that due to the background. Thus, the background concentration is overestimated by an amount depending on the target's concentration, size and location. High target concentrations, large targets, and targets located near sources or detectors result in significant overestimates of the background concentration, thus distorting the reconstructed images.

The addition of noise distorted the reconstructed images in a noise–level–dependent manner (Figure 6). Results shown in Figure 6 demonstrate that reasonable qualitative accuracy was obtained from the improved algorithm even for 10% Gaussian noise added to the detector readings. The quantitative estimate of $\gamma\sigma_{T,1\to 2}N_0$ is not satisfactory because of the noise. The mean lifetime values, however, are acceptable for up to 5% noise, even if the quantitative estimate of $\gamma\sigma_{T,1\to 2}N_0$ is incorrect. This is reasonable because $\gamma\sigma_{T,1\to 2}N_0$ is used only to delineate the target from the background. Its quantitative value is not important, because it is factored out in the mean lifetime reconstruction when computing the ratio of imaginary to real parts.

The images reconstructed from background–dominant signals did not show a uniform distribution of the background lumiphore but a four–lobed pattern (Figure 5), which is a consequence of the underdeterminedness of the inverse problem and the ill–conditioning of the weight matrix. Unlike the noise effect, whose influence is distributed through the reconstruction (Figure 6 and [8]), this pattern was observed in early iterations and may or may not improve after more iterations, depending on which algorithm was used. This poses a problem for image reconstruction when background lumiphore is present, because it prevents us from using early reconstruction results, which is an advantage of an iterative algorithm.

The improved algorithm works well for uniformly distributed background lumiphore and one isolated target, as demonstrated in this paper. What about more complicated objects, with nonuniform background lumiphore and multiple targets? First, the maximum possible concentration principle is always a useful tool to make a reasonable estimate of the lower bound for the range constraints, and is definitely better than blindly setting the lower bound to zero. For multiple targets or larger targets which strongly distort the estimate of MPC, an iterative update of the MPC may be used to remove the influence of the targets. That is, after reconstructing the targets from the current estimate of the MPC, a new MPC can be estimated using detector readings minus signal from the current reconstructed target, and used in the next reconstruction.

7. References

1. D. Y. Paithankar and E. M. Sevick–Muraca, "Fluorescence lifetime imaging with frequency–domain photon migration measurement," *OSA Trends in Optics and Photonics on Biomedical Optical Spectroscopy and Diagnostics*, E. M. Sevick–Muraca and D. Benaron, eds., vol. 3 (Optical Society of America, Washington, DC 1996), pp. 184–193.

2. M. A. O'Leary, D. A. Boas, X. D. Li, B. Chance, and A. G. Yodh, "Fluorescence lifetime imaging in turbid media," *Optics Letters*, vol. 21, pp. 158–160, 1996.

3. J. Chang, H. L. Graber, and R. L. Barbour, "Luminescence optical tomography of dense scattering media," *J. Opt. Soc. Am. A*, vol. 14, pp. 288–299, 1997.

4. D. C. Youla, "Mathematical theory of image reconstruction by the method of convex projections," *Image Recovery: Theory and Application,* Henry Stark, ed., Academic Press, New York, NY, 1987.

5. J. Chang, H. Graber, R. L. Barbour, and R. Aronson, "Recovery of optical cross section perturbations in dense scattering media using transport theory based imaging operators and steady–state simulated data and laser measurements," *Applied Optics* , vol. 35, pp. 3963–3978, 1996.

6. J. Chang, H. L. Graber, and R. L. Barbour, "Imaging of fluorescence in highly scattering media," *IEEE Trans. Biomed. Eng.* (in press)

7. J. Chang, W. Zhu, Y. Wang, H. L. Graber, and R. L. Barbour, "A regularized progressive expansion algorithm for recovery of scattering media from time–resolved data," *J. Opt. Soc. Am. A*, vol. 14, pp. 306–312, 1997.

8. J. Chang, H. L. Graber, and R. L. Barbour, "Dependence of optical diffusion tomography image quality on image operator and noise," in *Proc. 1995 IEEE Medical Imaging Conference*, (San Francisco, Oct. 1995), pp. 1524–1528.

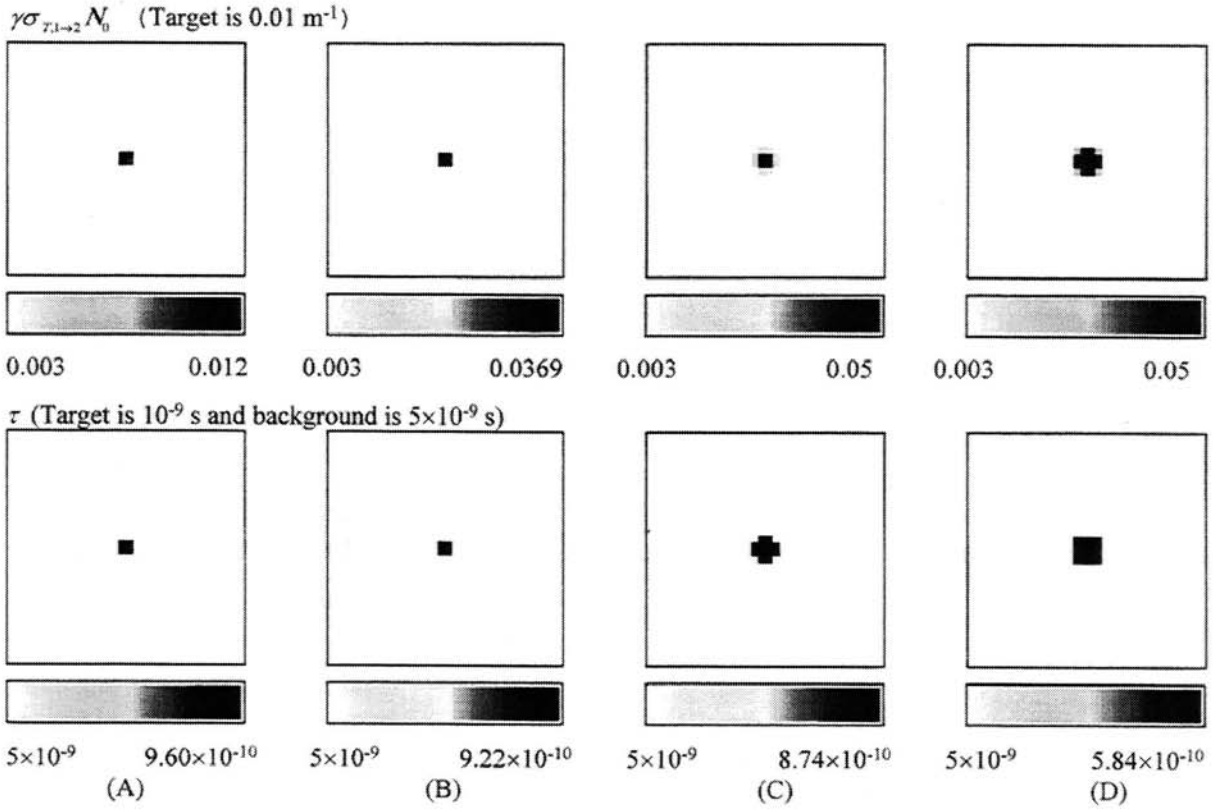

Figure 4. Reconstruction results with background–to–target ratio of 0.2 and different target sizes, using the improved algorithm with constraints.

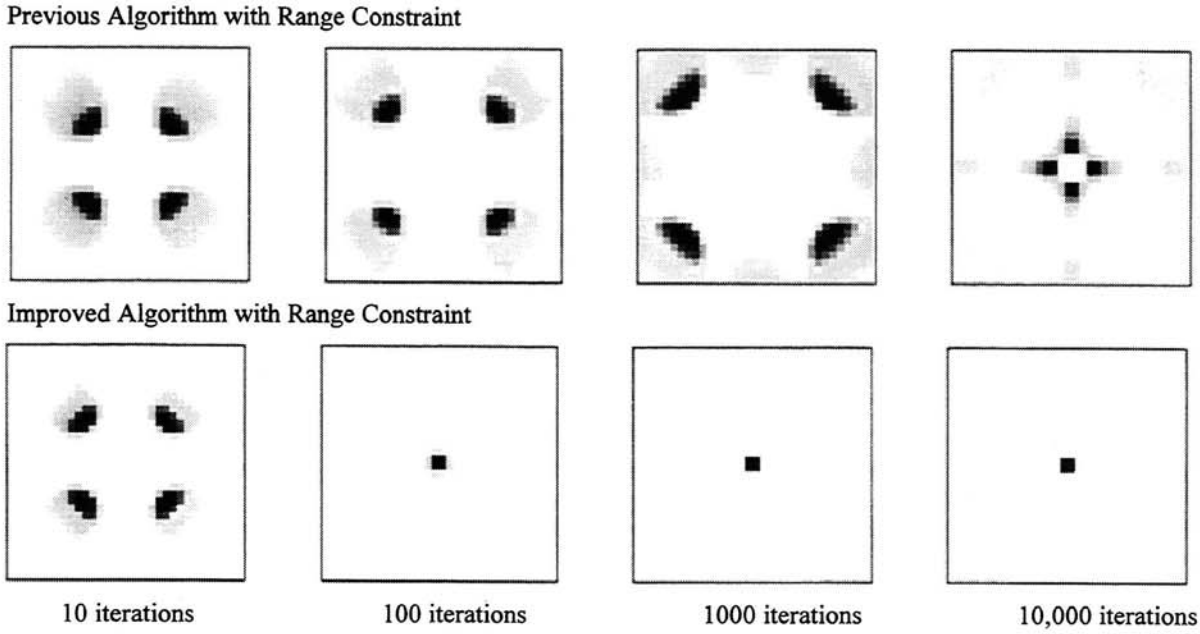

Figure 5. Comparison of reconstructions using the previous and improved algorithms with background–to–target lumiphore concentration ratio of 0.01.

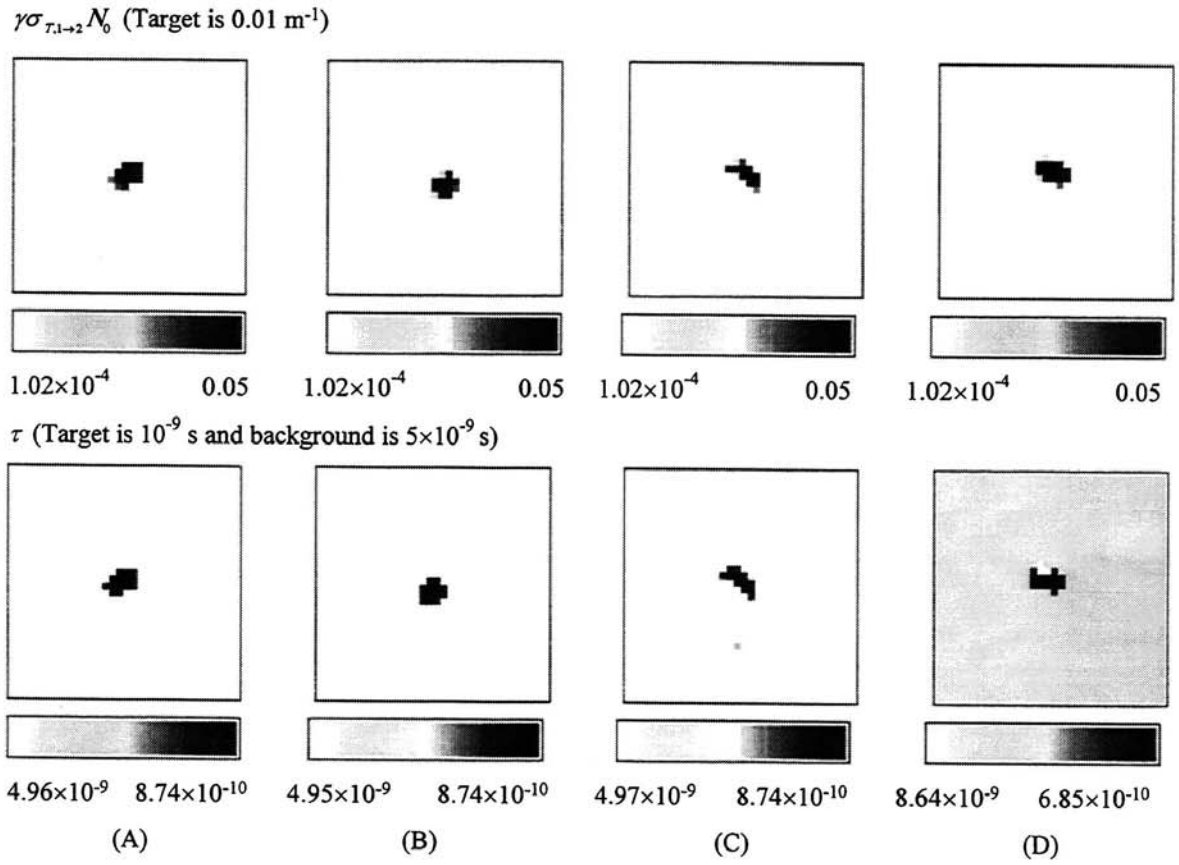

Figure 6. Reconstruction results with background–to–target ratio of 0.01 and different added noise level with target size 2.0 cm×2.0 cm, using the improved algorithm with constraints. (A) 1.0%, (B) 3.0%, (C) 5.0%, and (D) 10.0% noise.